IL NUOVO CIMENTO **47 C** (2024) 223
DOI 10.1393/ncc/i2024-24223-8

COLLOQUIA: HADRON2023

Heavy-flavour hadronization in ultra-relativistic heavy-ion collisions: From AA to pp

S. PLUMARI(1)(2)(*), V. MINISSALE(1)(2), Y. SUN(3) and V. GRECO(1)(2)

(1) *Department of Physics and Astronomy "E. Majorana", University of Catania Via S. Sofia 64, 1-95123 Catania, Italy*
(2) *Laboratori Nazionali del Sud, INFN-LNS - Via S. Sofia 62, I-95123 Catania, Italy*
(3) *School of Physics and Astronomy, Shanghai Key Laboratory for Particle Physics and Cosmology, and Key Laboratory for Particle Astrophysics and Cosmology (MOE), Shanghai Jiao Tong University - Shanghai 200240, China*

received 21 December 2023

Summary. — The Λ_c/D^0 ratio observed in AA collisions at RHIC and LHC energies have a value of the order of the unity. On the other hand, the recent experimental measurements in pp collisions at both $\sqrt{s} = 5.02\,\text{TeV}$ and $\sqrt{s} = 13\,\text{TeV}$ have shown ratios for charm baryons/mesons Λ_c/D^0 and Ξ_c/D^0 larger than those measured and expected in elementary e^+e^- collisions. We present a hadronization mechanism based on the coalescence and fragmentation processes and we show that this model gives a consistent description of several observables involving heavy-flavour hadrons from AA collisions to pp collisions. The results obtained within this approach suggest that a description of charmed hadron production in pp collisions require the assumption of the formation of a hot QCD matter at finite temperature. Finally, extending this approach to study the production of hadrons containing multiple charm quarks, Ξ_{cc}, Ω_{cc} and Ω_{ccc} we provide the predictions of multi-charmed hadrons in different collision systems, like Pb+Pb, Kr+Kr, Ar+Ar and O+O.

1. – Introduction

The main goal of the ongoing heavy-ion collisions program at Relativistic Heavy-Ion Collider (RHIC) and Large Hadron Collider (LHC) is the characterization of the state of matter created in these collisions, named Quark-Gluon Plasma (QGP). Many probes have been proposed to achieve this scope and among them the heavy quark hadron production have been considered one of the most useful probes to characterize QGP [1-3].

(*) E-mail: salvatore.plumari@dfa.unict.it

The large mass of Heavy Quarks (HQs) imply that they are produced by pQCD processes with a formation time $\tau_0 < 0.08$ fm/c $\ll \tau_{QGP}$ that permits to probe initial stage of the collision [4-6]. On the other hand, this large mass implies a larger thermalization time compared to the lifetime of the fireball produced, therefore HQs can probe the whole evolution of the plasma and conserve memory of the history of the system evolution to the final hadrons [7-16]. The study of Heavy-Flavour (HF) production can provide information about heavy-flavor transport coefficients in the QGP and at the same time can give information about the hadronization mechanism. In recent years, the experimental data on charmed hadrons have shown an enhancement of the charmed baryon/meson ratio similar to the one observed for light and strange hadrons, and larger than the one expected in collision systems as e^+e^-, $e^{\pm}p$ [17]. The recent experimental observation seems to indicate that in smaller collision systems, like proton-proton and proton-nucleus collisions, the heavy-flavour production is strongly consistent with the formation of a Hot QCD matter [18,19]. From the theoretical point of view, recently this analysis has been extended to bottom hadrons in pp collisions [20] and to multi-charmed hadrons [21, 22] in different collisions systems.

2. – Hadronization by coalescence and fragmentation

The coalescence model is one of the possible microscopic descriptions for the hadronization process in QGP. This model was able to explain the baryon-to-meson spectra and the splitting of elliptic flow of light and heavy mesons and baryons produced in heavy-ion collisions at top RHIC and LHC energies [23, 24] recently predicting a large $\Lambda_c/D^0 \sim 0.5$–1 in AA collisions [25, 26]. In this section we recall the basic elements of the coalescence model. The momentum spectrum of hadrons composed by N_q quarks can be written as

$$\frac{\mathrm{d}N_H}{\mathrm{d}y\mathrm{d}^2P_T} = g_H \int \prod_{i=1}^{N_q} \frac{\mathrm{d}^3p_i}{(2\pi)^3 E_i} p_i \cdot \mathrm{d}\sigma_i f_{q_i}(x_i, p_i) f_H(x_1 \ldots, p_1 \ldots) \delta^{(2)} \left(P_T - \sum_{i=1}^{n} p_{T,i} \right), \tag{1}$$

where g_H is the statistical factor to form a colorless hadron from quarks and anti-quarks. The $\mathrm{d}\sigma_i$ denotes an element of a space-like hypersurface while f_{q_i} are the quark (anti-quark) phase-space distribution functions for i-th quark (anti-quark) and $f_H(x_1 \ldots x_{N_q}, p_1 \ldots p_{N_q})$ is the Wigner function which describes the spatial and momentum distribution of quarks in a hadron. For $N_q = 2$ the above formula describes meson formation, while for $N_q = 3$ the baryon one. The Wigner function adopted has a Gaussian shape in space and momentum, $f_H(\ldots) = \prod_{i=1}^{N_q-1} A_W \exp\left(- \frac{x_{ri}^2}{\sigma_{ri}^2} - p_{ri}^2 \sigma_{ri}^2 \right)$, where x_{ri} and p_{ri} are the 4-vectors for the relative coordinates and A_W is a normalization constant fixed to guarantee that in the limit $p \to 0$ all the charm quarks hadronize by coalescence. The widths σ_{ri} of $f_H(\ldots)$ are related to the size of the hadron by the root mean square charge radius of the meson, for details see refs. [18, 26]. In our approach a charm quark with $p_T \neq 0$ can hadronize in two ways either by coalescence or by fragmentation. Using the hadronization probability $P_{coal}(p_T)$ to hadronize by coalescence one can associate a finite probability to hadronize by fragmentation according to the probability $P_{frag}(p_T) = 1 - P_{coal}(p_T)$. Finally, the hadron momentum spectra from fragmentation is given by $\frac{\mathrm{d}N_{had}}{\mathrm{d}^2p_T\,\mathrm{d}y} = \sum \int \mathrm{d}z \frac{\mathrm{d}N_{fragm}}{\mathrm{d}^2p_T\,\mathrm{d}y} \frac{D_{had/c}(z,Q^2)}{z^2}$ where $D_{had/c}(z, Q^2)$ is the fragmentation function and $z = p_{had}/p_c$ is the momentum fraction of heavy quarks transfered to the

final heavy hadron. In the calculations shown the Peterson fragmentation function is used [27].

3. – Charmed hadrons from AA to pp collisions

As shown in [26] at RHIC energies the coalescence plus fragmentation approach predicts for D meson with $p_T < 3$–4 GeV a similar contribution from coalescence and fragmentation. The model predicts a different behaviour at LHC energies where fragmentation plays a dominant role to the D-meson production because of the large number of minijet at higher collision energies. At higher p_T, the D-meson production is dominated by fragmentation mechanism at both energies. This different behaviour between coalescence and fragmentation produces a baryon enhancement that corresponds to an enhancement of the Λ_c production for $p_T < 3$–4 GeV at both RHIC and LHC energies. Therefore, in AA collisions this model predicts a rise and fall of the baryon/meson ratio. In the left and middle panels of fig. 1 the comparison between RHIC and LHC for the Λ_c/D^0 ratio is shown. We observe a reduction of the baryon/meson ratio between RHIC and LHC energies. This behaviour is mainly due to the larger number of minijets at LHC with respect to RHIC, where Λ_c baryons get a larger contribution from fragmentation leading to a smaller Λ_c/D^0 ratio compared to the one at RHIC. On the other hand, as shown in the right panel of fig. 1, the coalescence plus fragmentation approach predicts in a natural way a system size dependence of the charmed baryon/meson ratio which is consistent with the recent experimental data available for pp collisions at LHC energies [28]. The calculations for pp collisions assume the formation of a QGP medium, like the one simulated in hydrodynamics and transport calculations [29, 30]. In pp collisions the results of coalescence plus fragmentation model are similar to the Statistical Hadronization Model (SHM) ones, within the uncertainties, in the case of D^0, D^+, D^* and Λ_c but exhibit a significant difference for Ξ_c and Ω_c considering statistical models with the same number of resonances [18, 31].

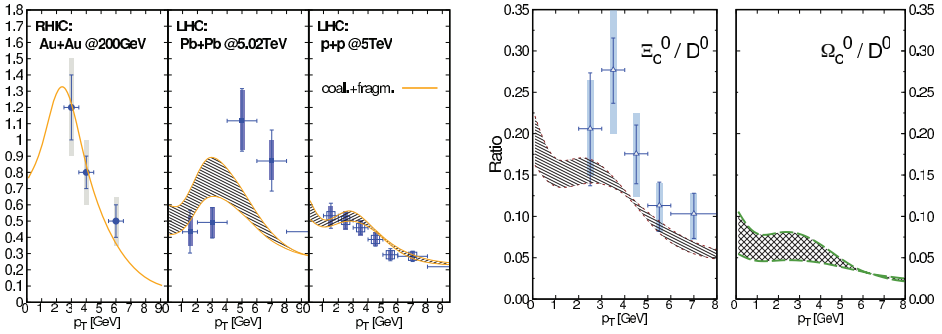

Fig. 1. – Left: Λ_c/D^0 ratio as a function of the transverse momentum at mid-rapidity for Au+Au at $\sqrt{s} = 200$ GeV [32] (left panel), for Pb+Pb at $\sqrt{s} = 5.02$ TeV [33] (middle panel) and p+p at $\sqrt{s} = 5$ TeV [28] (right panel). Right: Ω_c/D^0 and Ξ_c/D^0 ratios as a function of the transverse momentum at mid-rapidity for p + p at $\sqrt{s} = 5$ TeV. Data taken from ref. [34]. The upper and lower limit of the bands correspond to the maximum and minimum value of the baryon/meson ratio obtained increasing and decreasing the Wigner function widths by 20%.

4. – Multi-charmed hadrons and systems size scan

In the left panel of fig. 2 the yields are shown for single- and multi-charmed hadrons in PbPb collisions for 0–10% centrality at mid-rapidity within coalescence plus fragmentation compared with the results for SHM considering an enhanced set of charmed baryons with respect to the ones listed by the PDG, as suggested in [21,31,35]. The orange band in the plot corresponds to the yields obtained with realistic distribution for the lower limit and the one obtained with thermal distribution for the upper limit. For multi-charmed baryons Ξ_{cc}, Ω_{cc} and Ω_{ccc} the coalescence plus fragmentation approach shows a large sensitivity to the underlying charm distribution function. In fact, assuming a thermalized charm distribution, the model predicts an enhancement of the yields w.r.t. the realistic distribution as shown by the upper and lower limit in the band. This behaviour is due to the fact that in a thermal distribution there is a larger number of charms in a small momentum region making the recombination mechanism easier with respect to a more realistic distribution. This property produces an enhancement in the final total yields, and therefore the yields of Ξ_{cc}, Ω_{cc} and Ω_{ccc} result more sensitive to the charm distribution function with respect to the single-charmed hadrons because of their quark content. In the right panel of fig. 2 the single- and multi-charmed hadrons production is shown in different collision systems, like Pb+Pb, Kr+Kr, Ar+Ar and O+O collision systems. For these systems the initial p_T distribution used is the one from FONLL calculations that evolves in a QGP medium described by a relativistic Boltzmann approach, for details of the calculation see ref. [22]. From large to small collision systems the lifetime of the fireball decreases and so does the time that a charm quark spends in the QGP. Therefore, in smaller collision systems, the final transverse momentum spectrum of charm quarks are flatter than the one, for example, in Pb+Pb collisions, see ref. [22]. In the right panel of fig. 2 the $\mathrm{d}N/\mathrm{d}y$ obtained by coalescence plus fragmentation for each species (different bands) is shown as a function of the size of the system $A^{1/3}$ in comparison with SHM results (open symbols). The upper limit of the band corresponds to a fully thermalized

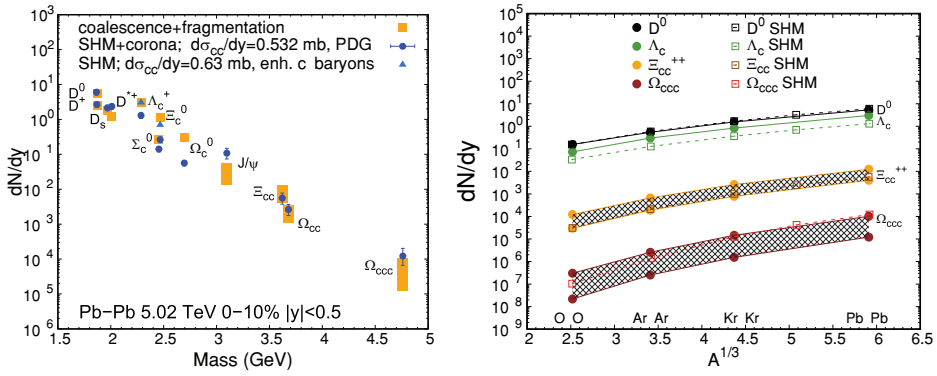

Fig. 2. – Left panel: charmed hadrons yields in PbPb collision at 5.02 TeV. The coalescence plus fragmentation results are shown by orange bands while the SHM results by blue open circles [21]. The band corresponds to the yields obtained with realistic distribution for the lower limit and the one obtained with thermal distribution for the upper limit. Right panel: $\mathrm{d}N/\mathrm{d}y$ at mid-rapidity of single- and multi-charmed hadrons as a function of the size of the systems. Different colors are for different species. Open symbols are for SHM calculation and full symbols are results obtained within coalescence plus fragmentation.

charm distribution while the lower limit is the result obtained using the charm distribution as obtained by solving the Boltzmann transport approach. The comparison with SHM shows that the $\mathrm{d}N/\mathrm{d}y$ have a similar but still different scaling with the decrease of the system size.

REFERENCES

[1] Dong X. and Greco V., *Prog. Part. Nucl. Phys.*, **104** (2019) 97.
[2] He M., van Hees H. and Rapp R., *Prog. Part. Nucl. Phys.*, **130** (2023) 104020.
[3] Andronic A. *et al.*, *Eur. Phys. J. C*, **76** (2016) 107.
[4] Das S. K., Plumari S., Chatterjee S., Alam J., Scardina F. and Greco V., *Phys. Lett. B*, **768** (2017) 260.
[5] Jiang Z.-F. *et al.*, *Phys. Rev. C*, **105** (2022) 054907.
[6] Chatterjee S. and Bozek P., *Phys. Lett. B*, **798** (2019) 134955.
[7] van Hees H., Mannarelli M., Greco V. and Rapp R., *Phys. Rev. Lett.*, **100** (2008) 192301.
[8] Gossiaux P. B. and Aichelin J., *Phys. Rev. C*, **78** (2008) 014904.
[9] Uphoff J., Fochler O., Xu Z. and Greiner C., *Phys. Lett. B*, **717** (2012) 430.
[10] Song T., Berrehrah H., Cabrera D., Cassing W. and Bratkovskaya E., *Phys. Rev. C*, **93** (2016) 034906.
[11] Cao S., Qin G.-Y. and Bass S. A., *Phys. Rev. C*, **92** (2015) 024907.
[12] Das S. K., Scardina F., Plumari S. and Greco V., *Phys. Lett. B*, **747** (2015) 260.
[13] Beraudo A., De Pace A., Monteno M., Nardi M. and Prino F., *JHEP*, **05** (2021) 279.
[14] Plumari S., Coci G., Minissale V., Das S. K., Sun Y. and Greco V., *Phys. Lett. B*, **805** (2020) 135460.
[15] Sambataro M. L., Sun Y., Minissale V., Plumari S. and Greco V., *Eur. Phys. J. C*, **82** (2022) 833.
[16] Sambataro M. L., Minissale V., Plumari S. and Greco V., arXiv:2304.02953 [hep-ph] (2023).
[17] Lisovyi M., Verbytskyi A. and Zenaiev O., *Eur. Phys. J. C*, **76** (2016) 397.
[18] Minissale V., Plumari S. and Greco V., *Phys. Lett. B*, **821** (2021) 136622.
[19] Beraudo A., De Pace A., Pablos D., Prino F., Monteno M. and Nardi M., arXiv:2306.02152 [hep-ph] (2023).
[20] He M. and Rapp R., *Phys. Rev. Lett.*, **131** (2023) 012301.
[21] Andronic A. *et al.*, *JHEP*, **07** (2021) 035.
[22] Minissale V., Plumari S., Sun Y. and Greco V., arXiv:2305.03687 [hep-ph] (2023).
[23] Greco V., Ko C. M. and Levai P., *Phys. Rev. Lett.*, **90** (2003) 202302.
[24] Minissale V., Scardina F. and Greco V., *Phys. Rev. C*, **92** (2015) 054904.
[25] Oh Y., Ko C. M., Lee S. H. and Yasui S., *Phys. Rev. C*, **79** (2009) 044905.
[26] Plumari S., Minissale V., Das S. K., Coci G. and Greco V.,, *Eur. Phys. J. C*, **78** (2018) 348.
[27] Peterson C., Schlatter D., Schmitt I. and Zerwas P. M., *Phys. Rev. D*, **27** (1983) 105.
[28] Acharya S. *et al.*, *Phys. Rev. C*, **104** (2021) 054905.
[29] Weller R. D. and Romatschke P., *Phys. Lett. B*, **774** (2017) 351.
[30] Greif M., Greiner C., Schenke B., Schlichting S. and Xu Z., *Phys. Rev. D*, **96** (2017) 091504.
[31] He M. and Rapp R., *Phys. Lett. B*, **795** (2019) 117.
[32] Adam J. *et al.*, *Phys. Rev. Lett.*, **124** (2020) 172301.
[33] Acharya S. *et al.*, *Phys. Lett. B*, **839** (2023) 137796.
[34] Acharya S. *et al.*, *JHEP*, **10** (2021) 159.
[35] He M. and Rapp R., *Phys. Rev. Lett.*, **124** (2020) 042301.